CFD flow modelling inside a three phase AC plasma torch working with air: influence of air radiation

Sabri Takali, Yann Cressault, Vandad-Julien Rohani, Frédéric Fabry, François Cauneau, Laurent Fulcheri

CFD flow modelling inside a three phase AC plasma torch working with air: influence of air radiation

Sabri Takali[(1)], Yann Cressault[(2)], Vandad Rohani[(1)], Frédéric Fabry[(1)], François Cauneau[(1)], Laurent Fulcheri[(1)]

[(1)] *MINES ParisTech, PSL-Research University, PERSEE Centre for processes, renewable energy and energy systems, rue Claude Daunesse, CS 10207, 06904 Sophia Antipolis Cedex, France,*
Tel : +33.493.957.540, Email: sabri.takali@mines-paristech.fr

[(2)] *Université Paul Sabatier, LAPLACE : Laboratoire Plasma et Conversion d'Energie, Toulouse III, 118 route de Narbonne, 31062 Toulouse cedex 09, France,*

Abstract: This work presents the heat and mass transfer modelling of 100 kW three phase AC plasma torch operating with air. The AC transient phenomena taking place in the arc region are simplified using a source model. A parametric study is performed to investigate the robustness of this simplification. The model includes gas and wall radiation. Results show the impact of radiation on the temperature field and wall heat losses.

Keywords: three phase plasma torch, source model, plasma radiation, wall heat flux

1. Introduction

Many MHD models have been developed for studying electric discharges in DC [1]–[3] and AC plasma torches [4]. Obtained results allowed a good assessment of arc behaviour and described carefully the role of the different phenomena governing the discharge but have always intersected with expensive calculus cost with a study domain limited to the inter-electrode zone. In order to simulate the whole torch domain including the solid components, a simplified source model is introduced hereafter.

2. Arc source model

The purpose of this work consists in predicting the plasma flow behaviour, quantifying thermal losses to the walls and analysing the interaction between the plasma gas and the different components of the torch. In order to obtain reliable results with a reduced computing cost, the following assumptions are considered:

i) The flow is stationary.

ii) The Local Thermodynamic Equilibrium (LTE) is assumed in the plasma which allows defining a unique temperature for all the present species in each point of the gas domain.

iii) The gas is incompressible since the Mach number is assumed below 0.3.

iv) For symmetry reasons, only one third of the torch is modelled.

2.1. The three phase AC plasma torch

The three phase AC plasma torch includes three graphite electrodes designed to operate in oxidizing conditions. As shown in Fig. 1, the simulation is limited to the components in contact with the air plasma: electrodes, electrical insulation, thermal insulation ceramic, stainless steel walls but also the water sheet that guarantees the cooling of the walls. This torch is designed for a 100 kWe nominal power and a 65 $Nm^3.h^{-1}$ air flow rate.

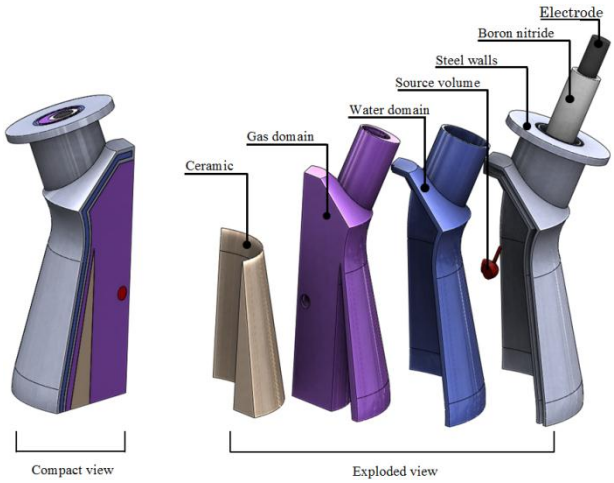

Fig. 1. Exploded view of the different domains in the model (one third of the torch)

2.2. Source model

The simplification of the arc column is mainly based on recent work of C. Rehmet, on the non-stationary MHD modelling of arc channel in plasma torches with multiple electrodes configurations working with a three phase AC power supply [4].

The shape and motion of the arc column depend of the different forces involved, mainly, hydrodynamic and electromagnetic forces. Although hydrodynamic forces influence the stability of the arc by implying continuous turbulence, magnetic forces at the electrode tips and along the arc column also play a major role.

Indeed, the arcs are characterized with electrode jets that accelerate the gas nearby the anode and cathode spots with velocities in the range of hundreds of $m.s^{-1}$, thus, forcing the arc column to be locally perpendicular to the electrode tip. The Maecker effect is behind this gas acceleration that happens due to the constriction of current flow section in the arc-electrode interface. The Maecker effect is hugely influenced by the electrode material and the spot temperatures [5]. For a current set at 400 A, MHD simulation predicts electrode jet speed neighbouring 360 $m.s^{-1}$ in a very small volume. Higher velocities could be reached for higher currents giving birth to shock waves in some circumstances. For the same current, the arc radius varies between 3 and 4 mm, the maximal temperature inside the arc is closed to 17 500 K and current density is about 5.10^7 $A.m^{-2}$ [6].

In the first hand, when the electrodes are in a planar configuration, the self-induced Lorentz forces along the arc column are minimal. In fact, the electrode jets tend to push the arcs toward the facing electrodes and since the Lorentz force have merely some deviating effects on a quasi-linear current conductor, the arc column remains confined within the inter-electrode space. On the other hand, when the electrodes are tilted relatively to the main axis, the electrode jets push the arc column away from the anode and the arc column is stretched further to reach the corresponding electrode driven by the electric potential in order to guarantee current continuity. This curvature is amplified by Lorentz force.

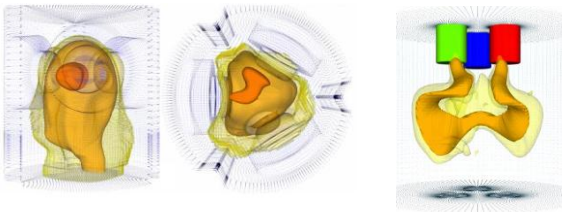

Fig. 2. (left and center) Arc represented with temperature iso-surfaces at 15 000 K, 10 000 K and 5 000 K in a planar electrode configuration, (right) arc represented with temperature iso-surfaces at 8 000 K and 5 000 K in parallel electrode configuration C. Rehmet [7].

Since the stationary assumption is considered, a simplified shape of the arc column will replace the time dependent shape. The chosen morphology intends to simplify the simulation while reproducing approximately the main phenomena involved in the inter-electrode volume.

Despite, the arcs have an erratic behaviour, some statistically preponderate profiles, such as the one represented in Fig. 2, have been observed both experimentally and through simulations. First, this morphology is simplified, by assuming that the arcs have the same diameter all over their length. Second, despite the discharge occurrence according to the current frequency, -with the rate of 6 arcs taking place each period between the 3 electrodes playing alternatively the role of anode and cathode, one at a time- we neglect the current frequency and assume that all the arcs coexist and occupy the same volume. The resulting shape according to Fig**. 3** is a tore like with arc roots linear to each electrode. This morphology is kept for the simulation as the source of power and momentum representative of the electromagnetic repulsive forces. The 100 kW power is injected homogeneously in this 4 cm^3 source domain and two components momentum is defined with an axial value of -800 $N.m^{-3}$ and a radial value of 4 000 $N.m^{-3}$ [8].

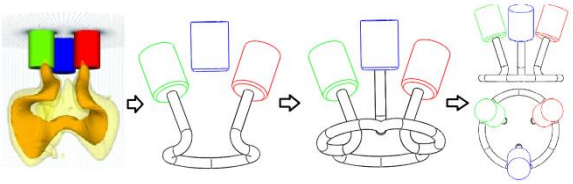

Fig. 3. schematic representation of the simplification process of the arc column (from the left to the right: statistically dominating shape of one arc according to MHD simulation, wire approximation (constant radius), stationary assumption (arcs coexistence), front and top views of the simplified arc column.

2.3. Simulation parameters and boundary conditions

The phenomena taken into account in this model are governed by the hydrodynamic Navier-Stokes equations, the RNG k-ε turbulence equations and the Radiation Transfer Equation (RTE). In RTE, the most important parameter is the absorption coefficient. Numerous spectral database of air absorption coefficients have been developed since 1960 [9]–[12]. In this simulation, we consider those resulting from the recent work of T. Billoux [13] which takes into account both atomic and molecular radiation contributions. This database is defined in the temperature range between 300 and 30 000 K and for the wavelengths from 0.209 µm to the far infrared. It considers radiation of molecular continuum (O_2, N_2, NO, O_3, NO_2, N_2O, NO_3, N_2O_5), atomic continuum (O, O^+, O^{2+}, O^{3+}, N, N^+, N^{2+}, N^{3+}, O^-), diatomic molecular bands (O_2, N_2, NO et N_2^+) and atomic radiation (6 217 for oxygen and 8 313 for nitrogen). The resulting Mean Absorption Coefficients are compared with those issued from the work of Bartlova et al. [14]. As shown in Fig. 4, the mean absorption coefficients of both databases have the same overall profile with pics placed at the same temperatures for the Rosseland and Planck averages. For the following simulations, we used this mean absorption coefficient defined on 6 bands covering the entire wavelength domain: [0.0333 – 0.402], [0.402 – 0.777], [0.777 – 1.013], [1.013 – 5.263], [5.263 – 8.108] and [8.108 - 100] µm.

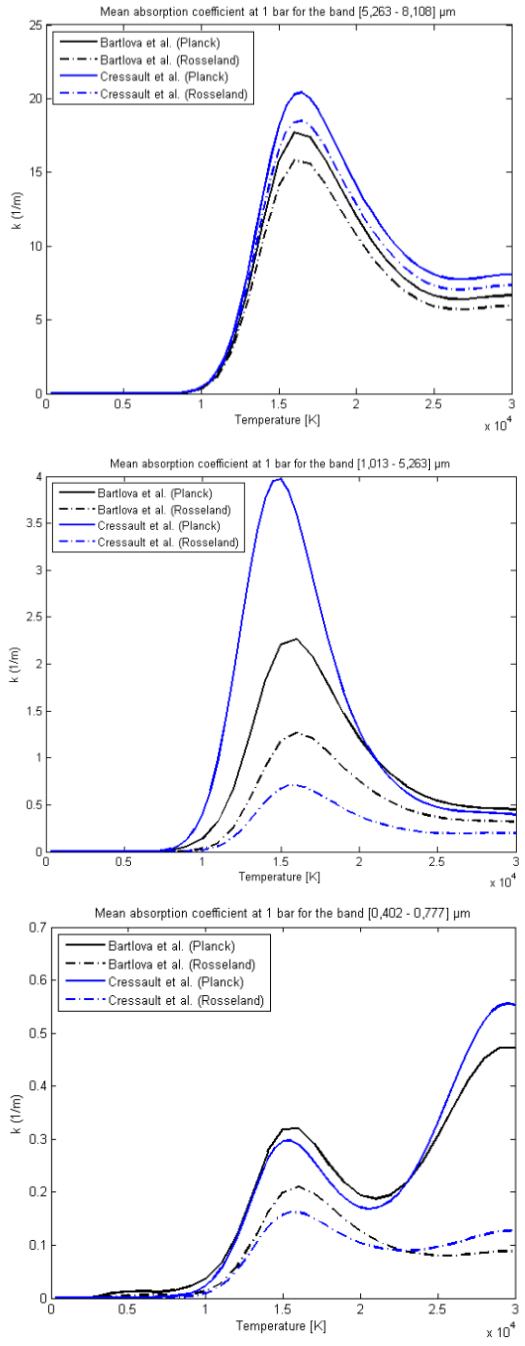

Fig. 4. Mean absorption coefficient of air at 1 bar for the following wave length intervals: [5.263 – 8.108], [1.013 – 5.263] and [0.402 – 0.777] µm

Concerning radiation implementation, the "Discrete Ordinate" model is selected with a spatial discretization of 3 polar angles and 2 azimuthal angles. For outer boundary conditions, the water cooling circuit is integrated to the model and a natural convection condition is fixed for the outer walls of the reactor.

3. Simulation results

3.1. Simulation of the air plasma flow without radiation

In order to verify the reliability of the source model approximation, the first simulations are conducted without radiation. Varying the source volume +/- 50 %, gives rise to few % temperature fluctuations downstream the source. Likewise, modifying +/- 10 % the momentum induces irrelevant variations on the results. Meanwhile, the change of the physical parameters shows the importance of tuning the operational parameters for better outlet conditions and for less thermal solicitation of the torch components. In fact, by reducing the air flow rate from 65 $N.m^3.h^{-1}$ to 25 $N.m^3.h^{-1}$, the inside walls overheat and the ceramic exceeds the maximum allowed temperature. Contrarily, when doubling the air flow rate, the outlet temperature field is less homogeneous and a small hot region is located in the center. In the other hand, when varying the power from 50 kW to 150 kW, results show a coherent increase of temperature and better homogenisation at the outlet without reaching critical temperature. The air sheeting blown between the ceramic and the steel walls plays its role and cools further the steel walls.

3.2. Simulation with radiation of gas and solid

As shown in Fig**. 5**, Fig. 6 and Table 1, radiation plays an important role in heat transfer. This is clear when we see the mass average temperature of the source volume passing from 11 241 K to 8 558 K when taking into account the radiation. Wall heat losses, initially negligible without radiation, reach also 17 % with radiation. Since the radiation term in the RTE is not linear, the effect of the source volume is investigated. Results show that varying the source volume by +/- 50 % induces a 6 % fluctuation of the gas maximum temperature and 10 % of the walls maximum temperature.

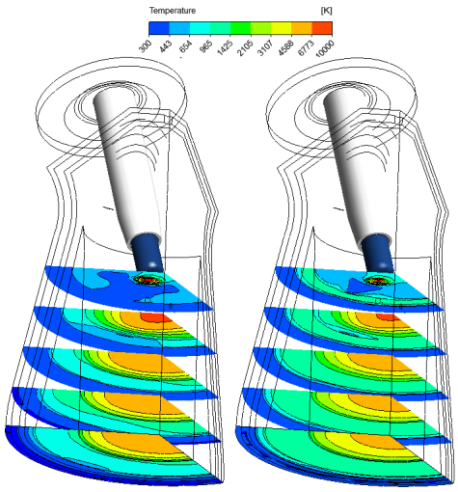

Fig. 5. Temperature field at different levels spaced by 4 cm without radiation (left) and with radiation (right)

Table 1. Comparison of temperature and heat flux of simulations with and without radiation

K°	Without Radiation			With Radiation		
	T_{min}	T_{moy}	T_{max}	T_{min}	T_{moy}	T_{max}
Arc zone	5205	11124	19635	4926	8558	10509
Gas	299	562	18869	299	690	9564
Water	299	300	301	299	303	344
Steel	299	301	310	299	373	474
Ceramic	305	732	1332	980	1187	1420
Electrode	479	897	2314	603	978	2138
Wall heat flux	0.1 kW ≈ 0.4 %			5.53 kW ≈ 16.7 %		

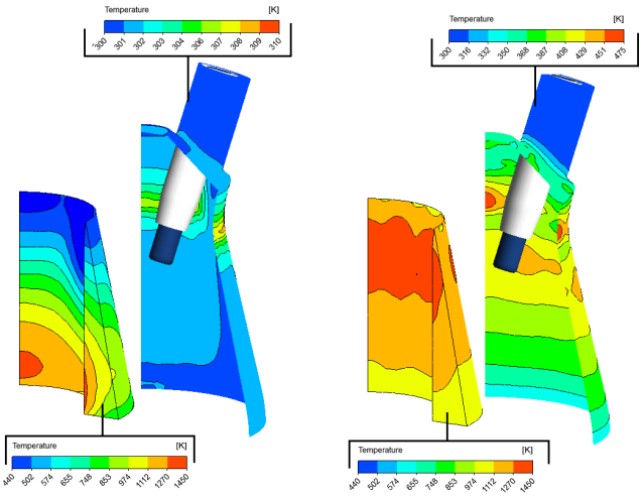

Fig. 6. Wall Temperature of the steel and the ceramic without radiation (left) and with radiation (right) (Different scales)

4. Conclusion

The stationary source model used to simulate the plasma air flow inside the torch leads to overall fair results with coherent sensitivity and trends versus modelling parameters. The introduction of radiation shows the important impact of this heat transfer mode on temperature distribution in the gas and on the surrounding walls. Simulations also demonstrated coherent sensitivity to operational parameters, mainly, power input and gas flow rate. The results showed that the temperatures of the different elements of the torch are in the operational range of the selected materials.

5. References

[1] H.-P. Li, E. Pfender, and X. Chen, Application of Steenbeck's minimum principle for three-dimensional modelling of DC arc plasma torches , *J. Phys. Appl. Phys.*, **36**, no 9, p. 1084, (2003)

[2] H.-P. Li and X. Chen, Three-dimensional modelling of a dc non-transferred arc plasma torch, *J. Phys. Appl. Phys.*, **34**, no 17, p. L99, (2001)

[3] B. Barthelemy, Combustion-Vitrification de déchets radioactifs par plasma d'arc : modélisation de la thermique et de la dynamique, *PhD thesis, Université de Limoges*, (2003)

[4] C. Rehmet, Étude théorique et expérimentale d'une torche plasma triphasée à arcs libres associée à un procédé de gazéification de matière organique, *PhD Thesis, Ecole Nationale Supérieure des Mines de Paris*, (2013)

[5] W. H. Gauvin, Some characteristics of transferred-Arc plasmas, *Plasma Chem. Plasma Process.*, **9**, no 1, p. 65-84, (1989)

[6] C. Rehmet, V. Rohani, F. Cauneau, and L. Fulcheri, 3D Unsteady State MHD Modeling of a 3-Phase AC Hot Graphite Electrodes Plasma Torch, *Plasma Chem. Plasma Process.*, **33**, no 2, p. 491-515, (2013)

[7] C. Rehmet, F. Fabry, V. Rohani, F. Cauneau, and L. Fulcheri, Unsteady state analysis of free-burning arcs in a 3-Phase AC plasma torch: comparison between parallel and coplanar electrode configurations, *Plasma Sources Sci. Technol.*, **23**, no 6, p. 065011, (2014)

[8] B. Ravary, Modélisation thermique et hydrodynamique d'un réacteur plasma triphase. Contribution à la mise au point d'un procédé industriel pour la fabrication de noir de carbone, *PhD thesis, Ecole Nationale Supérieure des Mines de Paris PARIS*, (1998)

[9] B. H. Armstrong, J. Sokoloff, R. W. Nicholls, D. H. Holland, and R. E. Meyerott, Radiative properties of high temperature air, *J. Quant. Spectrosc. Radiat. Transf.*, **1**, no 2, p. 143-162, (1961)

[10] J. Meyerott, Absorption coefficient of air, p. 104, (1960)

[11] D. R. Churchill, B. H. Armstrong, and K. G. Mueller, Absorption coefficient of heated air: Compilation to 24,000 K, **2**, (1965)

[12] B. Peyrou, L. Chemartin, P. Lalande, B. G. Chéron, P. Rivière, M.-Y. Perrin, and A. Soufiani, Radiative properties and radiative transfer in high pressure thermal air plasmas, *J. Phys. Appl. Phys.*, **45**, no 45, p. 455203, (2012)

[13] T. Billoux, Elaboration d'une base de données radiatives pour des plasmas de type CwHxOyNz et application au transfert radiatif pour des mélanges air, CO2 et CO-H2, *PhD thesis, Université Toulouse III - Paul Sabatier*, (2013)

[14] N. Bogatyreva, M. Bartlova, and V. Aubrecht, Mean absorption coefficients of air plasmas, *J. Phys. Conf. Ser.*, **275**, no 1, p. 012009, (2011)

Acknowledgment

Authors would like to thank M. Bartlova for providing air radiation data.